Electronic Supplementary Material (ESI) for ChemComm.

Supporting Information

Detection and Tracking of Cytoplasmic G-Quadruplexes in Live Cells

Lu-Si Rao, Liang Hao, Liu-Yi Liu, You-Liang Zeng, Bing-Bing Liang, Wenting Liu,* and Zong-Wan Mao*

Key Laboratory of Bioinorganicand Synthetic Chemistry of Ministry of Education, School of Chemistry, IGCME, Sun Yat-Sen University, Guangzhou 510275, China.

E-mail: liuwenting@mail.sysu.edu.cn, cesmzw@mail.sysu.edu.cn

Experimental Procedures

General synthetic procedures. All chemicals were purchased from commercial sources and used as received unless otherwise indicated. ^{1}H-NMR, ^{13}C-NMR and ^{31}P-NMR spectra were recorded on a Bruker Advance 600 spectrometer (Germany). Shifts were referenced relative to the internal solvent signals. Elemental analysis (C, H, N) was carried out using an Elemental Vario EL CHNS analyzer (Germany). ESI-MS spectra were recorded on a Thermo Finnigan LCQ DECA XP spectrometer (USA). The quoted m/z values represented the major peaks in the isotopic distribution.

Compound **TPPA** (tris(4-(pyridin-4-yl)phenyl)amine, tris(4-(pyridine-4 -)phenyl)amine) and **IBTPP** ((4-iodobutyl)triphenylphosphonium iodide) were prepared as described.[1]

TTPP (4,4',4 "-(nitrilotris(benzene-4,1-diyl))tris(1-(4-(triphenylphosphonio)butyl)pyridin-1-ium) iodide) synthesis method:

The synthesis route diagram is shown. Weigh 100 mg (i.e. 0.21 mmol) **TPPA** and 1.20 g (i.e. 2.10 mmol) **IBTPP** in a single-mouth round-bottom flask, and add 10 mL DMF (N, N '-dimethyl-formamide) into the reaction flask with a measuring cylinder. Dissolve and mix the reactants with a magnetic agitator. After the oil bath was heated to 100 ℃ on the magnetic stirring heater in advance, the reaction bottle was placed in the oil bath at 100 ℃ and stirred under nitrogen protection for 72 hours, and the color of the solution was dark red and black. The target final product was obtained by pumping and filtration/centrifugation, and then washed with ice ether for three times and dried, and finally orange-red solid was obtained.

TPPA: **^{1}H-NMR** (400 MHz, DMSO-d_6): δ 8.62 (d, J = 6.2 Hz, 6H), 7.84 (d, J = 8.7 Hz, 6H), 7.72 (d, J = 6.3 Hz, 6H), 7.24 (d, J = 8.7 Hz, 6H). **^{13}C-NMR** (151 MHz, DMSO-d_6): δ 150.00, 148.02, 147.37, 132.22, 128.81, 124.94, 121.33. **ESI-MS** (m/z): [**TPPA**+H]$^{+}$ calcd. for $C_{33}H_{25}N_4^{+}$, 477.59, found: 477.35; [**TPPA**+2H]$^{2+}$ calcd. for $[C_{33}H_{26}N_4]^{2+}$, 239.30, found: 239.22.

IBTPP: **^{1}H-NMR** (600 MHz, DMSO-d_6): δ 7.92 (ddt, J = 8.8, 4.8, 1.7 Hz, 3H), 7.80 (dddd, J = 18.7, 11.9, 6.6, 2.6 Hz, 12H), 3.62 (ddd, J = 16.2, 11.1, 7.2 Hz, 2H), 3.35 (t, J = 6.9 Hz, 2H), 1.96 (p, J = 7.0 Hz, 2H), 1.64 (h, J = 7.9 Hz, 2H). **^{13}C-NMR** (151 MHz, DMSO-d_6): δ 135.45 (d, J = 3.2 Hz), 134.06 (d, J = 10.2 Hz), 130.76 (d, J = 12.4 Hz), 118.88, 33.82, 23.10 (d, J = 3.8 Hz), 19.70, 7.61. **^{31}P-NMR** (243 MHz, DMSO-d_6): δ 24.03. **ESI-MS** (m/z): [**IBTPP**−I]$^{+}$ calcd. for $C_{22}H_{23}P^{+}$, 445.30; found: 445.34.

TTPP: **^{1}H-NMR** (600 MHz, DMSO-d_6): δ 9.02 (d, J = 7.4 Hz, 6H), 8.50 (d, J = 6.3 Hz, 6H), 8.17 (d, J = 8.4 Hz, 1H), 7.94 – 7.75 (m, 45H), 7.39 (d, J = 8.4 Hz, 6H), 4.59 (t, J = 5.5 Hz, 6H), 3.66 (d, J = 14.6 Hz, 6H), 2.14 (t, J = 7.7 Hz, 6H), 1.62 (m, 6H). **^{13}C-NMR** (151 MHz, DMSO-d_6): δ 154.01, 149.52, 145.07, 135.51, 134.12, 130.79, 129.28, 125.44, 124.21, 119.03, 118.47, 64.60, 59.08, 31.79, 20.33, 19.17. **^{31}P-NMR** (243 MHz, DMSO-d_6): δ 23.95.

Materials. All chemicals were purchased from commercial sources and used as received without further purification. HSA (Human Serum Albumin, Sigma-Aldrich), BSA (Bovine Serum Albumin, Sigma-Aldrich), ctDNA (Deoxyribonucleic acid sodium salt from calf thymus, Sigma-Aldrich), RNA (yeast) (Ribonucleic acid from torula yeast, Sigma-Aldrich), Coumarin 307 (Sigma-Aldrich), PDS (Pyridostatin trifluoroacetate salt, Sigma-Aldrich), LTR (LysoTracker Red, Invitrogen™) and MTR (MitoTracker Red, Invitrogen™) were used as received.

DNA sample preparation. The oligonucleotides were purchased from Invitrogen (Shanghai, China) with PAGE or HPLC purification. The sequence of the nucleic acids used see Table S1. G-quadruplex DNA structures were forming by an annealing process (heating at 95 ℃ for 5 min and then slowly cooling to room temperature overnight) in buffer. DNA concentration was measured by Nanodrop 200/200c (Thermo Science).

Photophysical properties. UV-Vis absorption spectra were obtained on a Varian Cary 300 spectrophotometer (USA). Emission spectra and lifetime measurements were performed on an Edinburgh FLS 920 spectrometer (UK). G-quadruplex DNA were prepared in 10 mM Tris-HCl buffer (pH 7.4, 100 mM KCl) with the concentration of 200 μM as DNA stock solutions.

The UV-Vis absorption spectra of **TTPP** (10 μM) was collected from 350 nm to 550 nm. For fluorescence emission spectra, **TTPP** (1 μM) was excited at 405 nm and emission was recorded from 420 to 800 nm.

For titration experiments, small aliquots of DNA stock solutions were successively added into the **TTPP** solution (1 μM) in 10 mM Tris-HCl buffer (pH 7.4, 100 mM KCl). The solution was stirred and allowed to equilibrate for at least 5 min before the emission spectra were measured. The fluorescence titrations data were analyzed by nonlinear fitting according to the independent-site model[2].

For time correlated-single photon counting (TCSPC) measurements, the decay curves of **TTPP** were excited with 405 nm pulsed excitation (500 ps fwhm) and monitored at 580 nm by emission spectra. The decay represents an average of 10,000 laser pulses. The decay curves of the instrument response function (IRF) were obtained by measuring the LUDOX scatterer. Decay traces were best fitted to a bi-exponential or tri-exponential decay model using the equation: $F(t) = A + B_1 \exp(-t/\tau_1) + B_2 \exp(-t/\tau_2)$ or $F(t) = A + B_1 \exp(-t/\tau_1) + B_2 \exp(-t/\tau_2) + B_3 \exp(-t/\tau_3)$.

For quantum yield experiment, the absorbance was approximately equal to the 0.05 at wavelengths above the excitation wavelength (405 nm) and emission was collected from 420 to 800 nm. The relative fluorescence quantum yields were determined using coumarin 307 in ethanol as the reference standard (Φ=0.56)[3] and were calculated from equation: $\Phi_x = \Phi_s \times (F_x/F_s) \times (A_s/A_x) \times (n_x/n_s)^2$, where Φ represents quantum yield; F is grated intensities (areas) of the emission spectrum; A is absorbance at the excitation wavelength; n is the refractive index of the solution; and the subscripts x and s refer to the unknown and the standard, respectively.

Molecular docking. DNA preparation: the structure of the DNA-ligand complex was downloaded from RCSB Protein Data Bank. The original ligand and water were removed by PyMOL[4] and the DNA was prepared by Accelrys Discovery Studio 2.5.5 for docking studies. Ligand preparation: the probe **TTPP** is optimized using DFT calculations by Gaussian09 package at B3LYP/6-31g (d, p) level. Using the optimized **TTPP** structure, the partial atomic charges were obtained by restrained electrostatic potential (RESP)[5] calculating with Gaussian 09 package at the level of HF/6-31g*. After that, the docking calculations were performed by the AutoDock 4 suite of programs[6], using ligand flexible docking approach that allows ligand flexibility. The Lamarckian genetic algorithm[7] was chosen as the search protocol using the default parameters except for number of GA runs (ga_run = 100) and the maximum number of energy evaluations (ga_num_evals = 25,000,000). The docking model with the lowest docked free energy was selected for further investigated in this article. And then, the docking complex was optimized with minimization protocols by Accelrys Discovery Studio 2.5.5 The displaying images were rendered with PyMOL or Accelrys Discovery Studio 2.5.5.

The hydrophobic contacts were presented by LigPlot$^+$ v.1.4.5 software[8] with hydrophobic-any contact distance 2.9-4.5.

Cell culture. A549, HLF and MCF-10A cells were obtained from Experimental Animal Center of Sun Yat-sen University (Guangzhou, China). Cells were maintained in DMEM (Dulbecco's modified Eagle's medium, Gibco BRL) or RPMI 1640 (Roswell Park Memorial Institute 1640, Gibco BRL) medium, containing 10% FBS (fetal bovine serum, Gibco BRL), 100 μg/mL streptomycin (Gibco BRL), and 100 U/mL penicillin (Gibco BRL). The cells were cultured at 37 ℃ with 5% CO_2/95% air (v/v) in humidified incubator. In each experiment, the reference group cells were treated with vehicle control (1% DMSO).

Cell viability assay. The cytotoxicity in the dark and phototoxicity of **TTPP** towards different cell lines was determined by MTT assay. For cytotoxicity in the dark, the cells were seeded in 96-well plates (Corning) and grown overnight. Then the cells were treated with series concentrations of **TTPP** and cisplatin. After incubation for 44 h, 20 μL MTT (3-(4,5-dimethylthiazol-2-yl)-2,5-diphenyltetrazoli-um bromide, Sigma) solution (5 mg/mL in PBS) was added to each well. The plates were incubated for an additional 4 h before the media was carefully removed, and DMSO was added (150 μL per well). After shaking for 5 min, the absorbance at 595 nm was measured using a microplate reader (Infinite M200 Pro, Tecan, Männedorf, Switzerland). Each experiment was repeated at least three times to get the mean values. For phototoxicity, the cells were incubated with the tested compounds for 12 h and then irradiated with a 425 nm LED light (40 mW cm^{-2}) for 15 min (36 J cm^{-2}). After another 32 h of incubation, MTT was added. The cytotoxicity was determined as described above.

Confocal microscopy. Confocal imaging of **TTPP** was performed using a confocal laser scanning microscope (LSM 880 NLO, Carl Zeiss, Göttingen, Germany) with a 63u oil-immersion objective lens. For live cell imaging experiments, A549 cells were incubated with **TTPP** (20 μM) at 37 °C for 24 h and then washed three times with ice-cold PBS and visualized by confocal microscopy. The wavelengths for one- and two-photon excitation of **TTPP** are 405 nm and 810 nm, respectively. Emission was collected at 580 ± 20 nm (**TTPP**). For colocalization

experiments, A549 cells were incubated with **TTPP** (20 μM) at 37 ℃ for 23.5 h and then further co-incubated with LTR (100 nM), MTR (100 nM) at 37 ℃ for 0.5 h. Cells were washed three times with ice-cold PBS and visualized by confocal microscopy immediately. The excitation and emission parameters of **TTPP** are consistent with the living cell imaging experiments. The excitation wavelength of LTR and MTR is 561 nm and the emission was collected at 590 ± 20 nm. For DNase or RNase digest experiments, A549 cells were incubated with **TTPP** (20 μM) at 37 °C for 24 h and then washed three times with ice-cold PBS, fixed with 4% paraformaldehyde in PBS (20 min at room temperature, 1 mL/well). The cells were then permeabilized using 0.1% Triton X-100 in PBS (1 mL/well) for 20 min at room temperature before being treated with 100 U/mL DNase I (Takara) or 100 μg/mL RNase A (Takara) for 2 h at 37 ℃. Cells were finally washed three times with PBS and visualized by confocal microscopy using the same parameters as in the live cell imaging experiment. Approximately 200 cells were used to the statistical analysis.

Fluorescence lifetime imaging microscopy (FLIM). FLIM imaging of **TTPP** was performed using Zeiss LSM 880 NLO multiphoton microscopes equipped with a bh TCSPC FLIM system (Becker & Hickl GmbH, Berlin, Germany). The two-photo excitation of samples was performed by femtosecond Ti:Sapphire laser (Coherent Chameleon) and the emission was collected using a Zeiss BiG-2 GaAsP detector. TCSPC module type is a SPC-150 module and the resolution of images is 512×512 pixel. For FLIM imaging, different cells were incubated with **TTPP** at 37 ℃ with different incubation times and concentrations, and then washed three times with ice-cold PBS and detected by FLIM system. The wavelength for two-photon excitation of **TTPP** is 810 nm and the emission records from 545 to 590 nm. The acquisition time was enough to obtain a better SNR. Lifetime data were fitted to a tri-exponential function for each pixel using SPC-Image software. The same settings and data processing method were used in different FLIM imaging experiments. For cell synchronization, cells were incubated for 24 hours in serum-free DMEM (G0/G1), grown for 16 hours in DMEM, 20% FBS and 200 mM mimosine (G1/S), and for three hours in DMEM and 10% FBS (S phase). For pyridostatin treatment experiments, A549 cells were incubated with **TTPP** (10 μM) at 37 ℃ for 18 h and then further co-incubated with different concentrations of pyridostatin (20 μM) at 37 °C for 6 h. For the cisplatin treatment experiments, A549 cells were co-incubated with **TTPP** (10 μM) and cisplatin (12.5 μM) at 37 ℃ for 24 h. For the erastin treatment experiments, A549 cells were incubated with **TTPP** (10 μM) at 37 ℃ for 12 h and then further co-incubated with erastin (10 μM) at 37 °C for 12 h. Cells were washed three times with ice-cold PBS and detected by FLIM system immediately.

Supplementary Figures

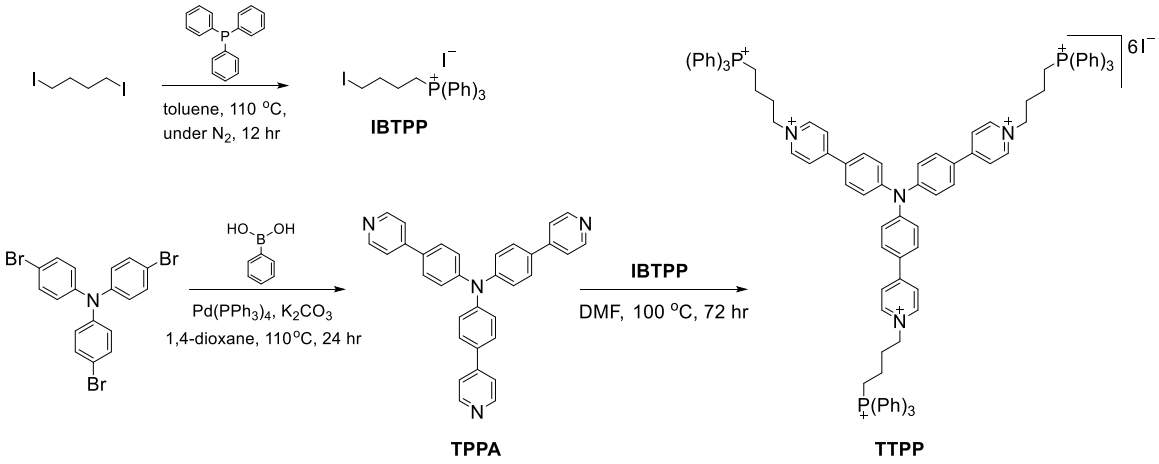

Figure S1. The synthetic reactions of the target product **TTPP**.

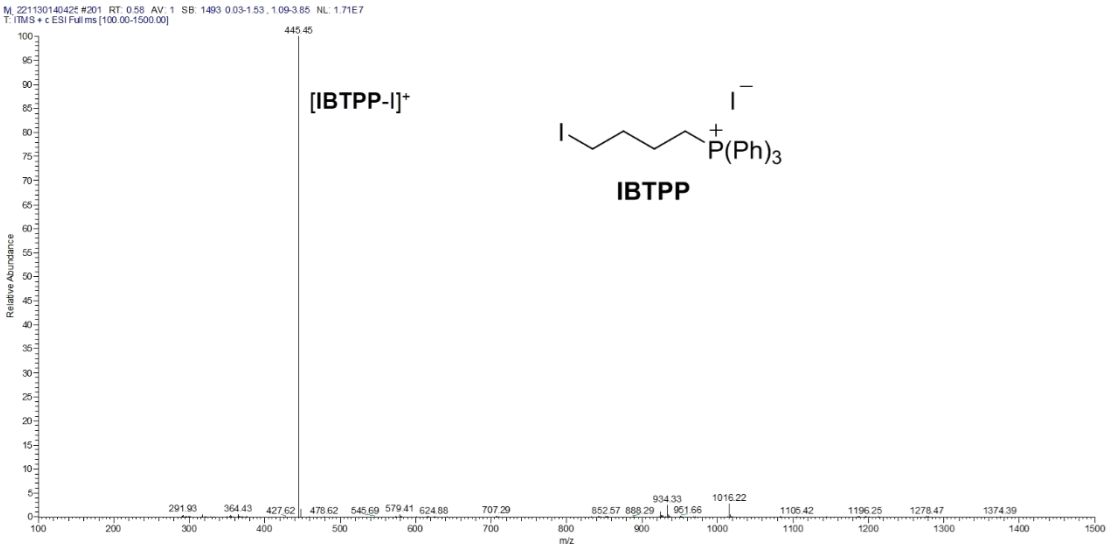

Figure S2. The ESI-MS spectrum of the intermediate product **IBTPP**.

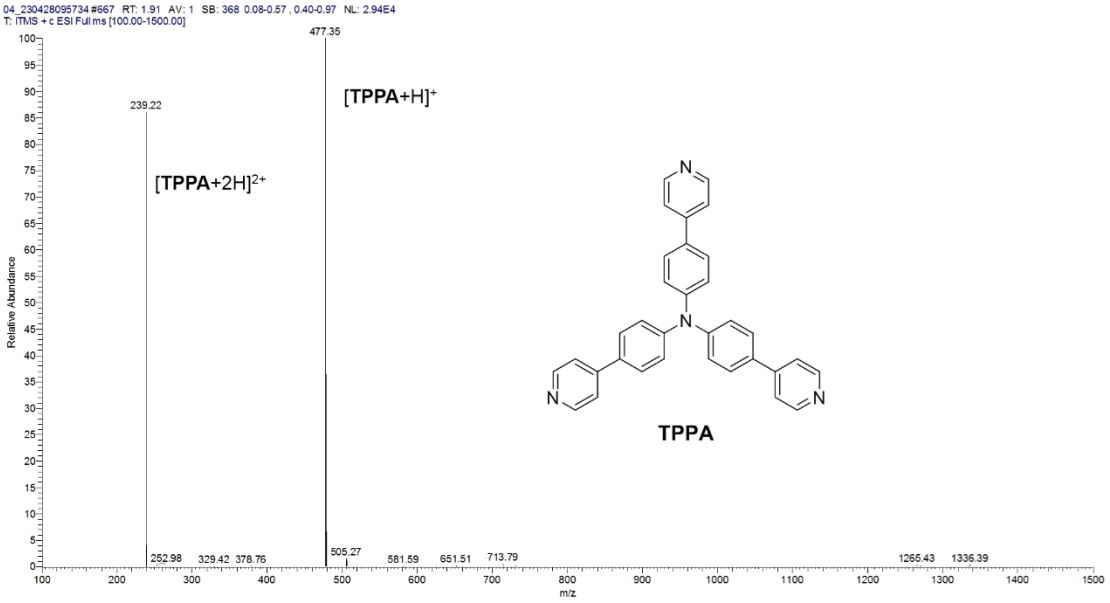

Figure S3. The ESI-MS spectrum of the intermediate product **TPPA**.

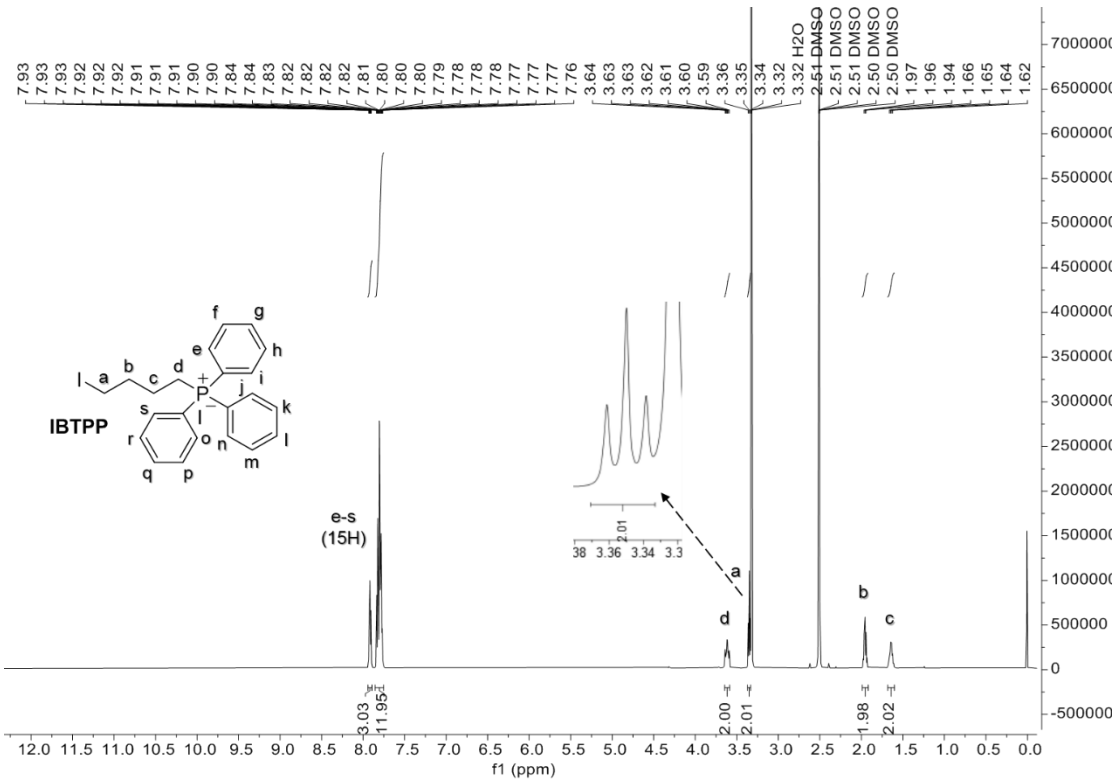

Figure S4. The ^{1}H-NMR (600 MHz) spectrum of the intermediate product **IBTPP** in DMSO-d_6.

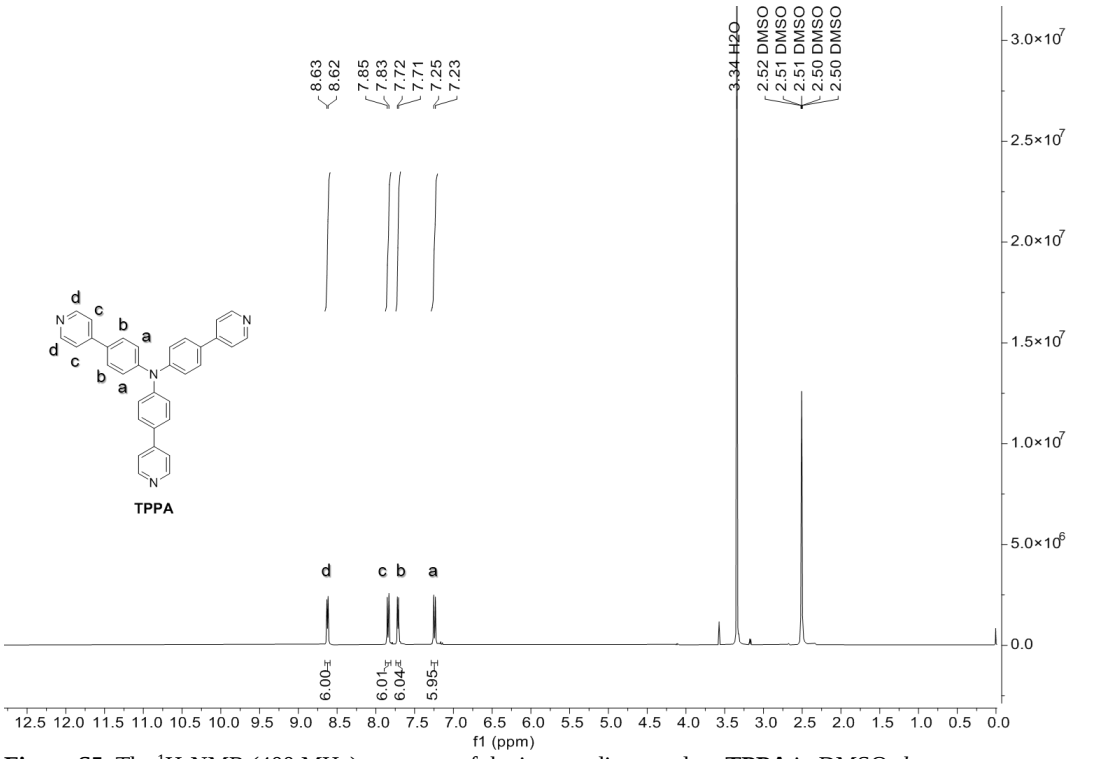

Figure S5. The [1]H-NMR (400 MHz) spectrum of the intermediate product **TPPA** in DMSO-d_6.

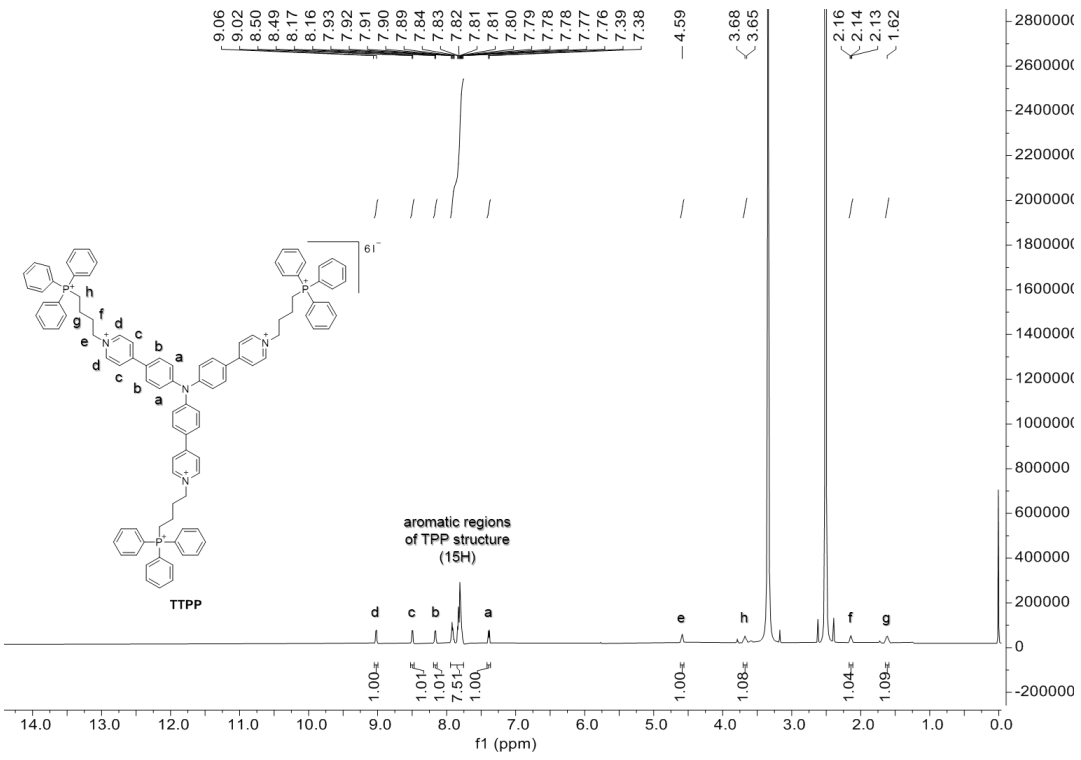

Figure S6. The [1]H-NMR (600 MHz) spectrum of the target product **TTPP** in DMSO-d_6.

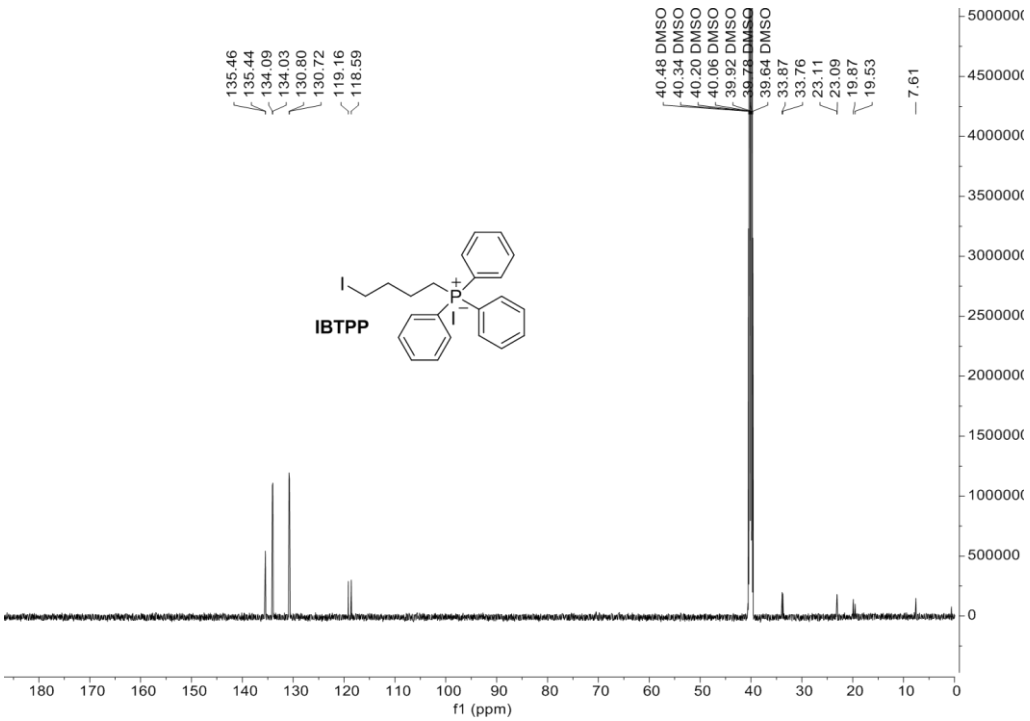

Figure S7. The ^{13}C-NMR (151 MHz) spectrum of the intermediate product **IBTPP** in DMSO-*d*$_6$.

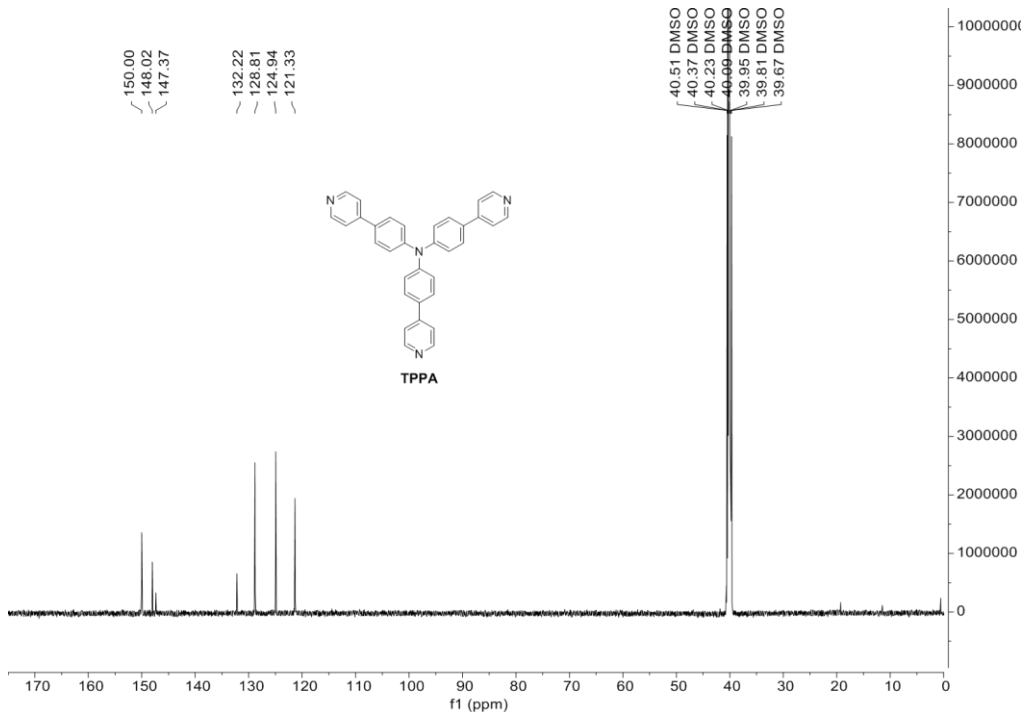

Figure S8. The ^{13}C-NMR (151 MHz) spectrum of the intermediate product **TPPA** in DMSO-*d*$_6$.

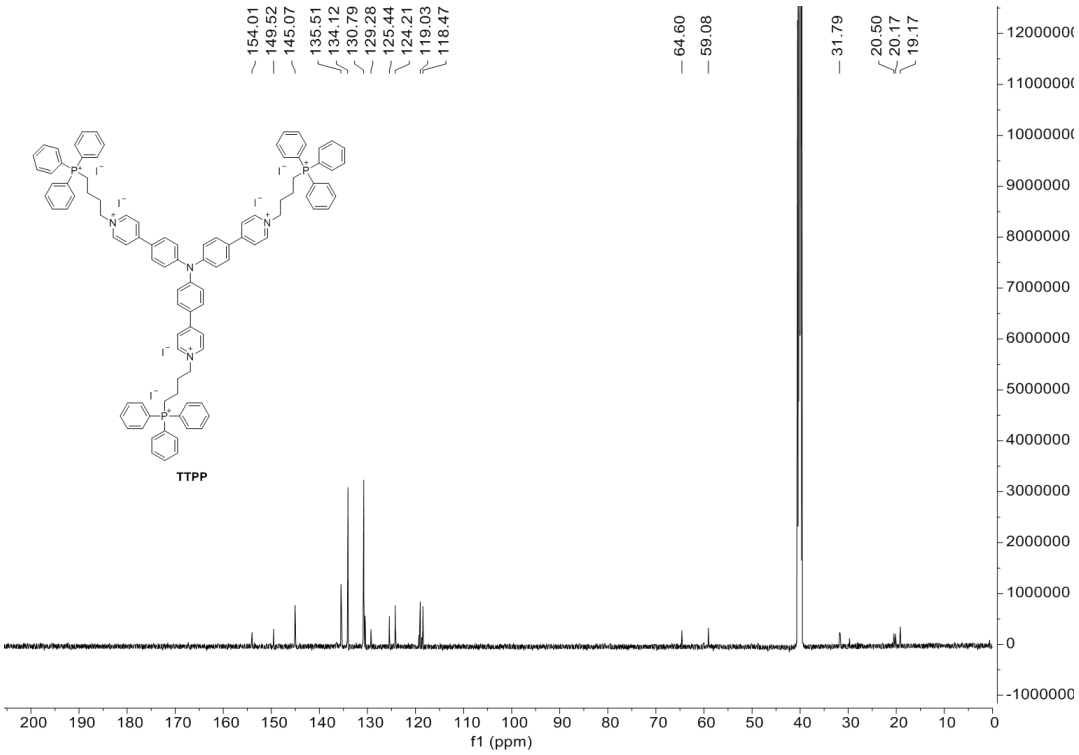

Figure S9. The ^{13}C-NMR (151 MHz) spectrum of the target product **TTPP** in DMSO-d_6.

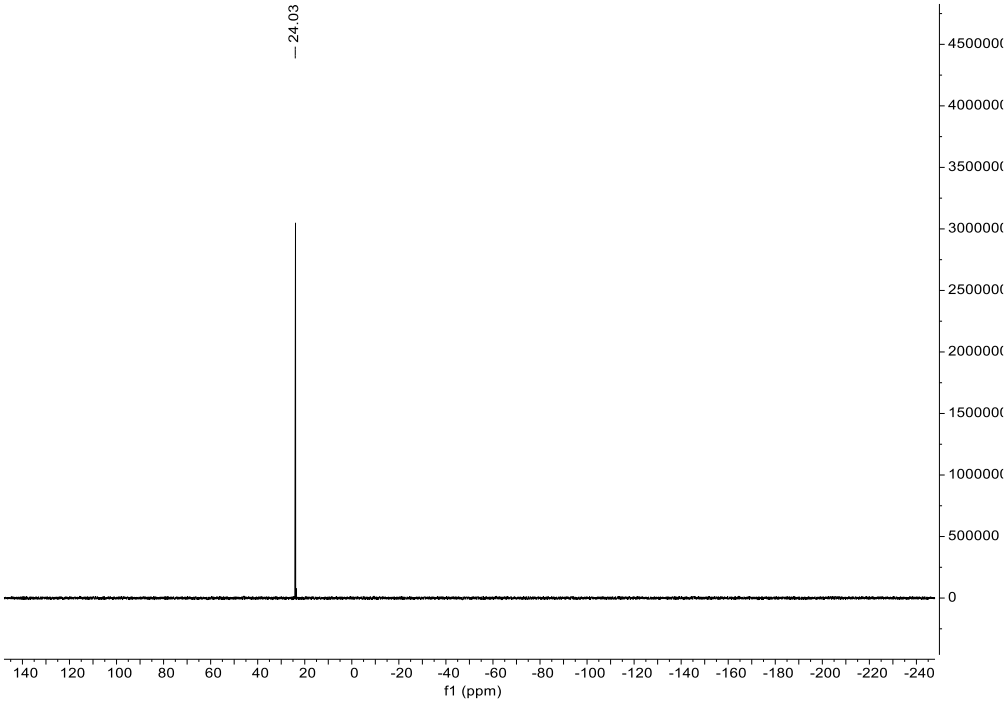

Figure S10. The ^{31}P-NMR (243 MHz) spectrum of the intermediate product **IBTPP** in DMSO-d_6.

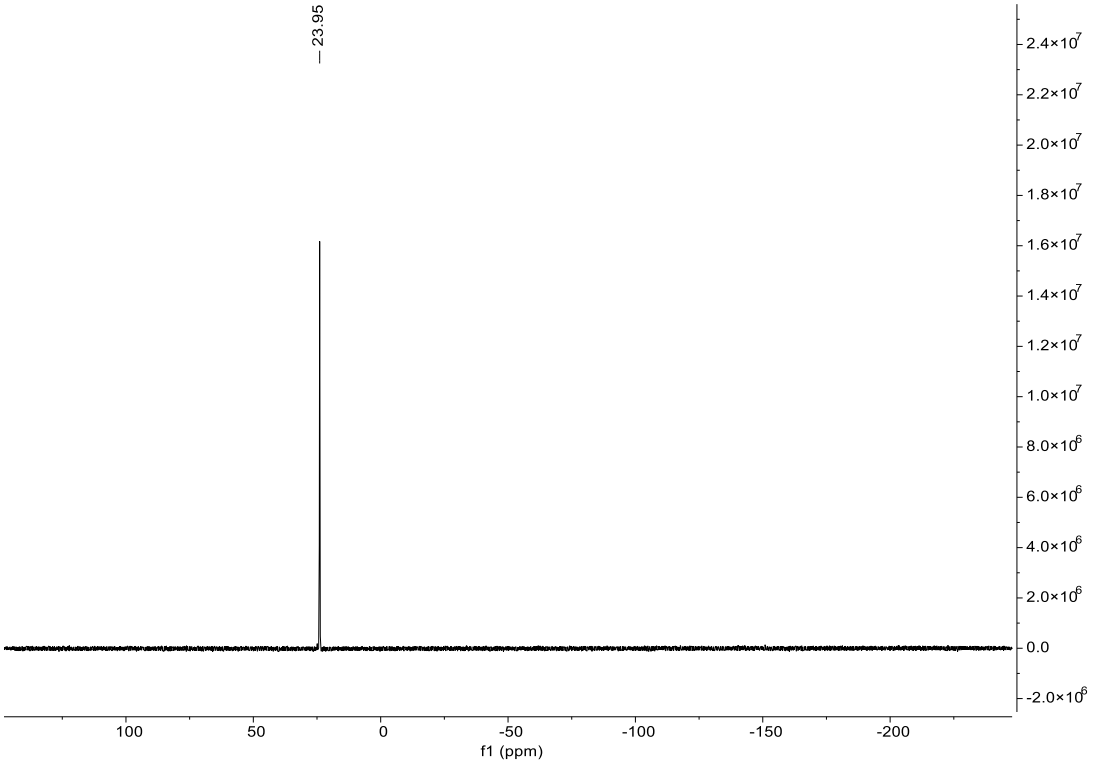

Figure S11. The ^{31}P-NMR (243 MHz) spectrum of the target product **TTPP** in DMSO-d_6.

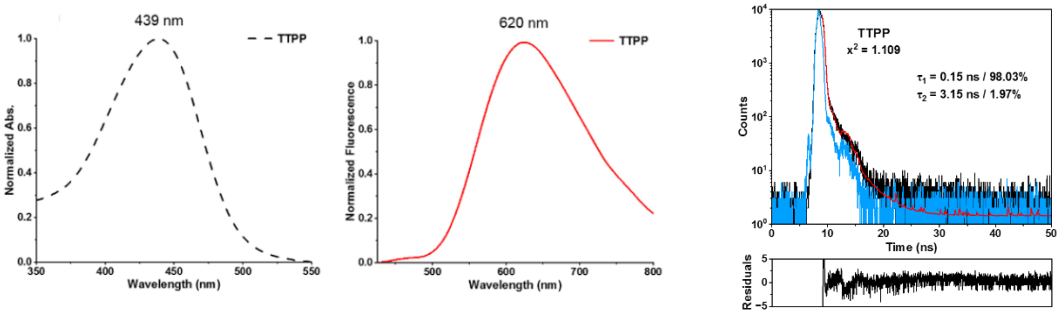

Figure S12. The normalized UV-Vis absorption spectra, fluorescence emission spectra and the fluorescence lifetime (decays) of **TTPP** in 10 mM Tris, 100 mM KCl, pH 7.4 at λ_{ex} = 405 nm. The fitting is corresponding to a bi-exponential decay model. Data traces, the instrument response (IRF) and fittings are shown in black, blue and red, respectively.

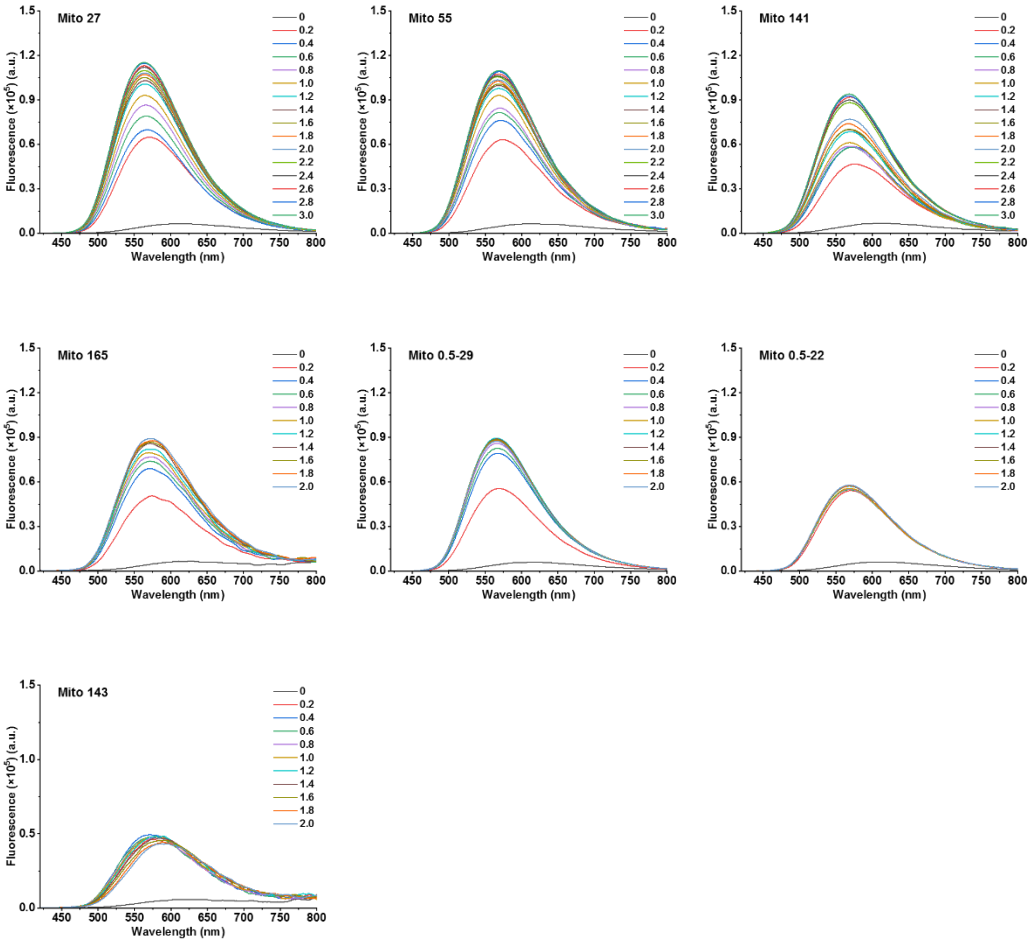

Figure S13. The fluorescence emission spectra of **TTPP** (1 μM) probe titrated by different mtDNA-G4s topologies in 10 mM Tris-HCl, 100 mM KCl, pH 7.4 at λ_{ex} = 405 nm. (Ratio = mtDNA-G4/**TTPP**)

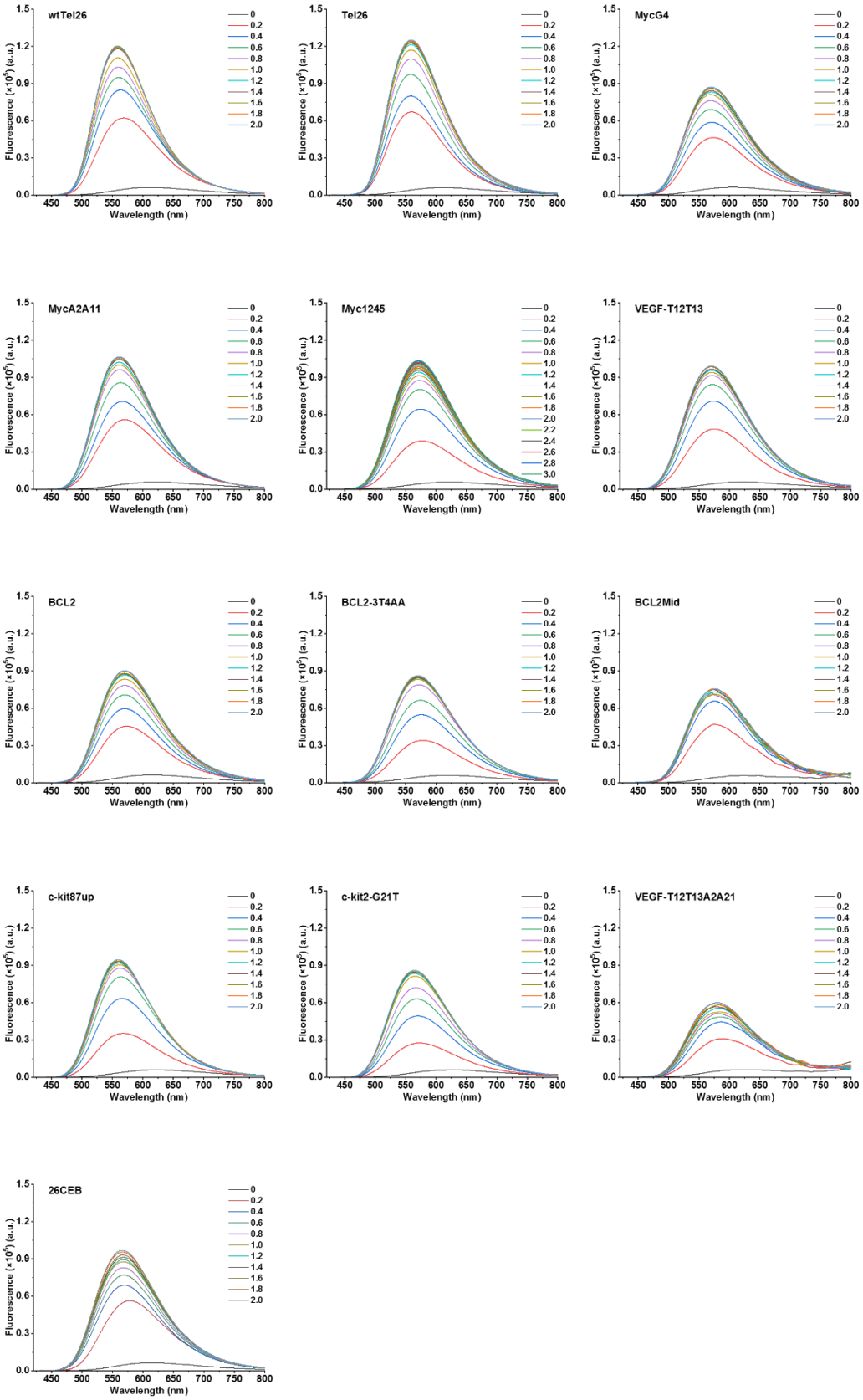

Figure S14. The fluorescence emission spectra of **TTPP** (1 μM) probe titrated by other monomeric DNA-G4s topologies in 10 mM Tris-HCl, 100 mM KCl, pH 7.4 at λ_{ex} = 405 nm. (Ratio = DNA-G4/**TTPP**)

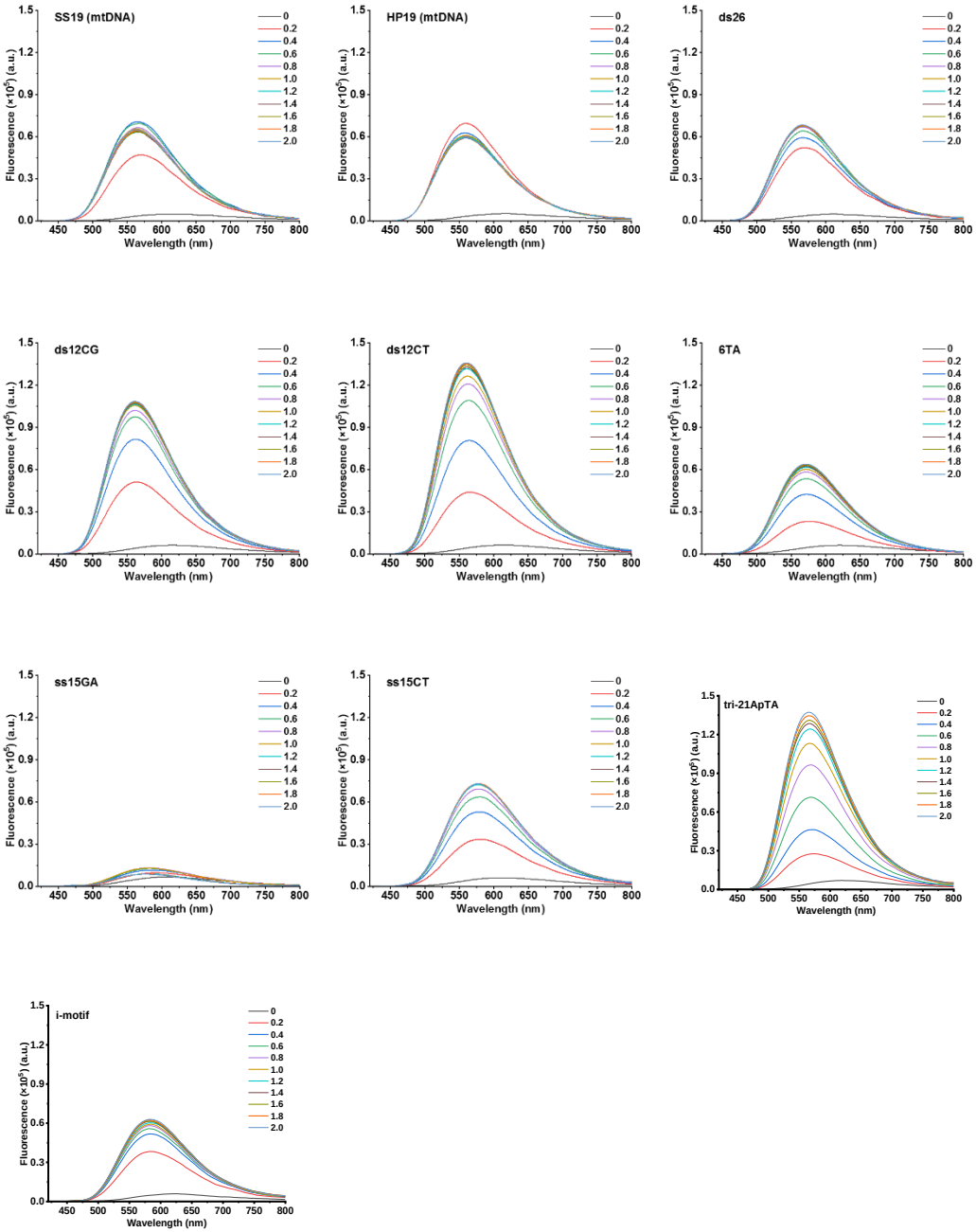

Figure S15. The fluorescence emission spectra of **TTPP** (1 μM) probe titrated by different non-G4s DNA topologies in 10 mM Tris-HCl, 100 mM KCl, pH 7.4 at λ_{ex} = 405 nm. (Ratio = non-G4 DNA /**TTPP**)

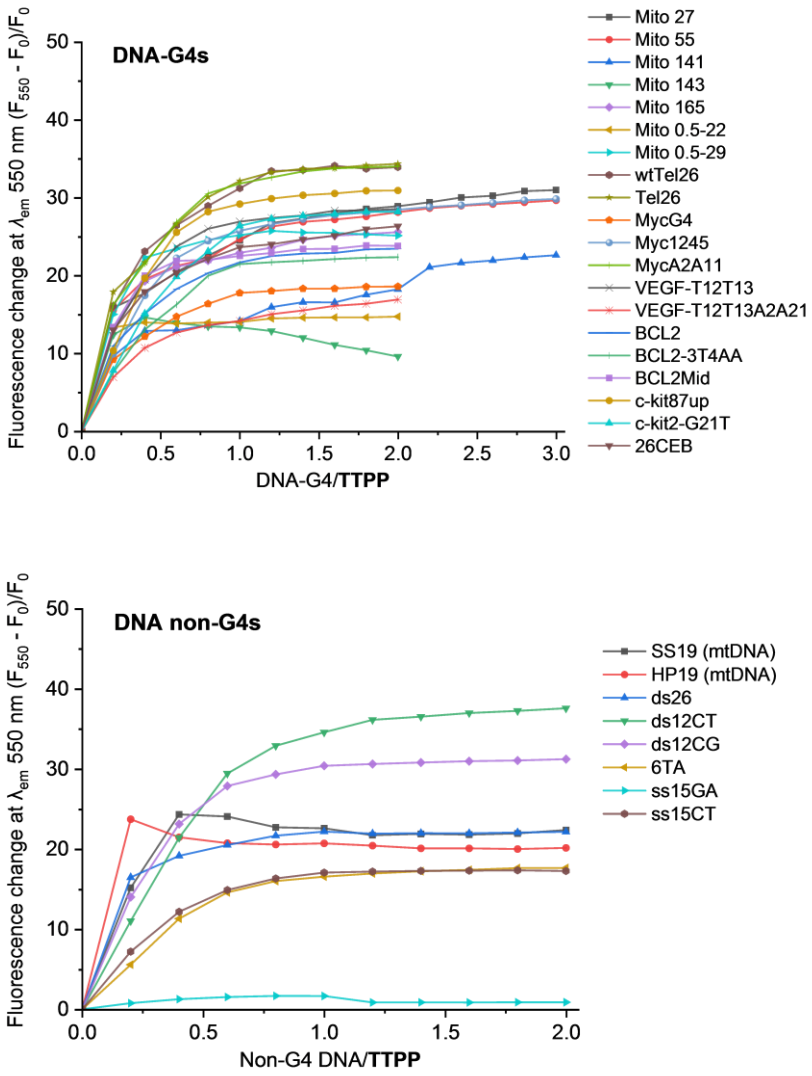

Figure S16. The fluorescence emission intensity changes at λ_{em} = 550 nm of **TTPP** probe (1 μM) titrated by different DNA topologies in 10 mM Tris-HCl, 100 mM KCl, pH 7.4 at λ_{ex} = 405 nm. (Ratio = DNA/**TTPP**)

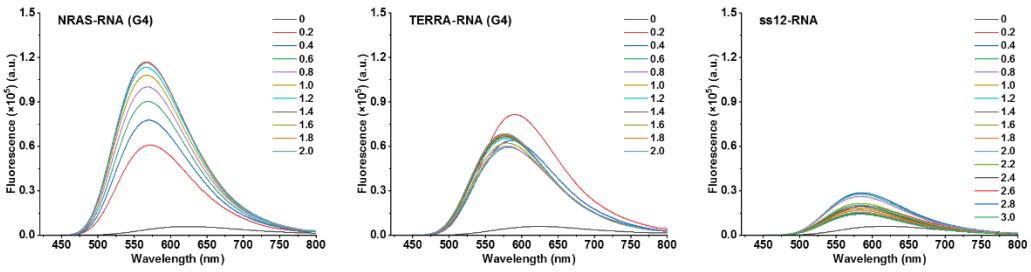

Figure S17. The fluorescence emission spectra of **TTPP** (1 μM) probe titrated by different RNA topologies in 10 mM Tris-HCl, 100 mM KCl, pH 7.4 at λ_{ex} = 405 nm. (Ratio = RNA/**TTPP**)

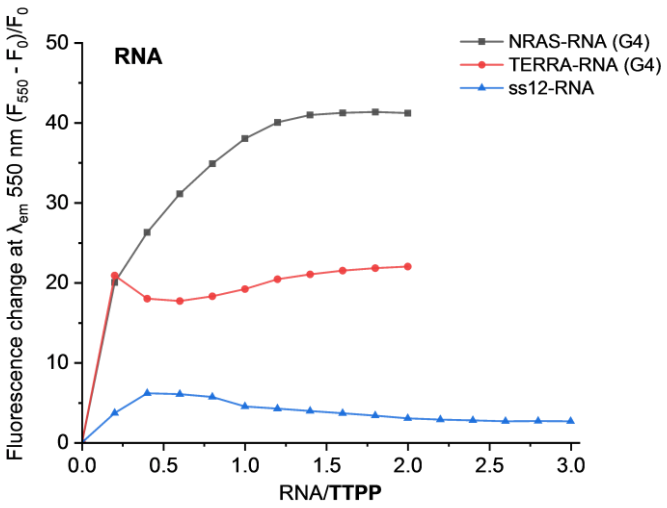

Figure S18. The fluorescence emission intensity changes at λ_{em} = 550 nm of **TTPP** probe (1 μM) titrated by different RNA topologies in 10 mM Tris-HCl, 100 mM KCl, pH 7.4 at λ_{ex} = 405 nm. (Ratio = RNA/**TTPP**)

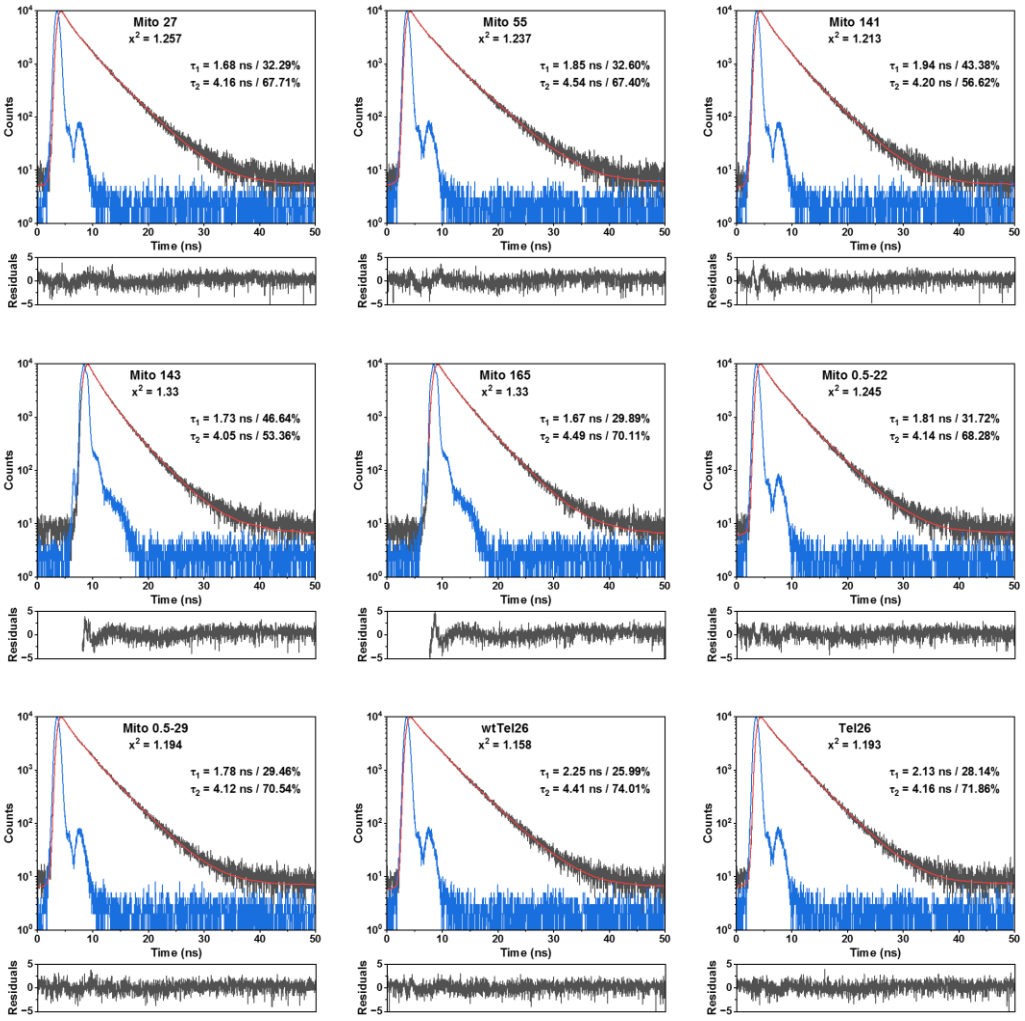

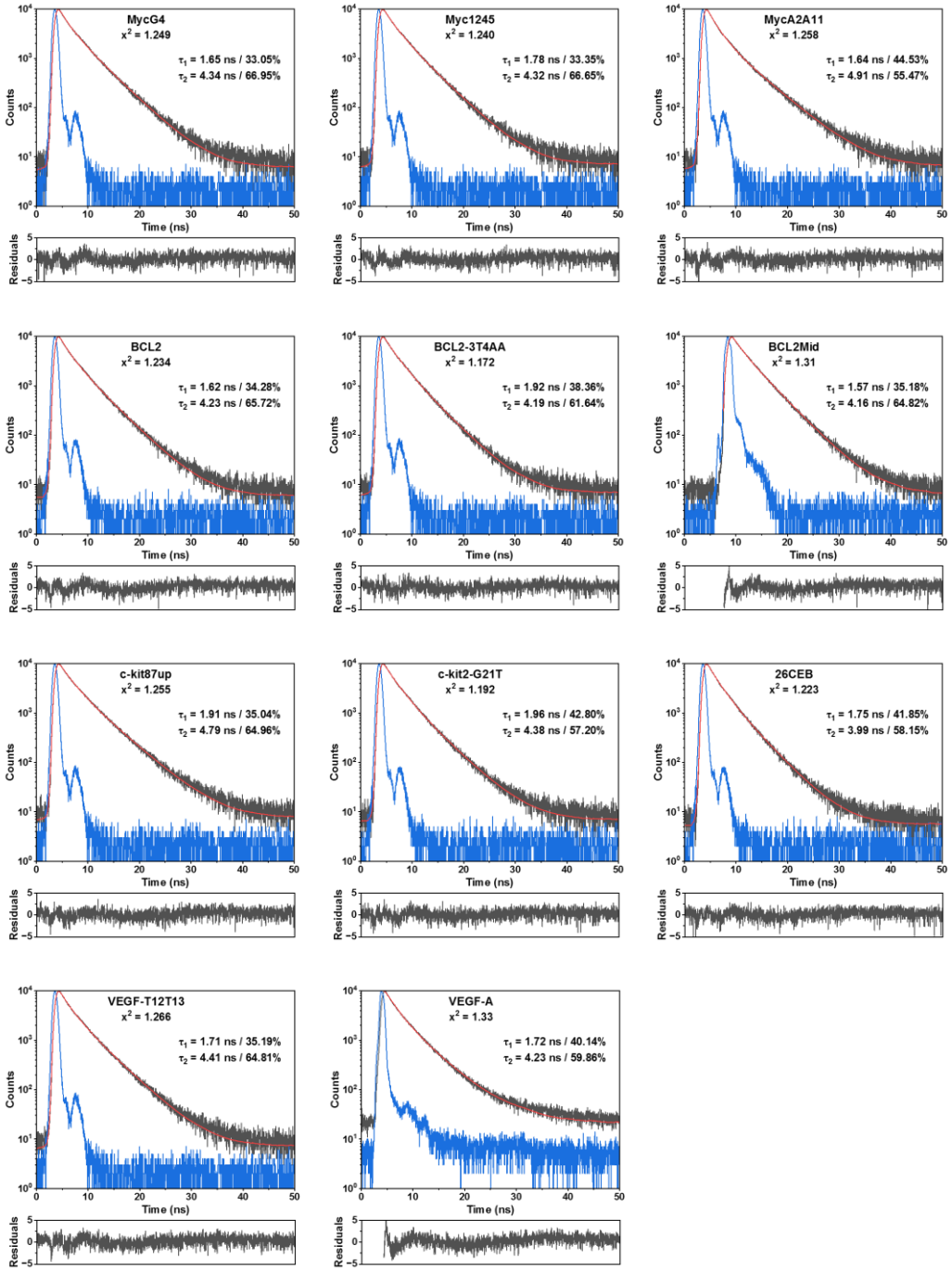

Figure S19. The fluorescence lifetimes (decays) of **TTPP** (1 μM) in the presence of different DNA-G4s topologies in 10 mM Tris-HCl, 100 mM KCl, pH 7.4. All fittings are fitted to a bi-exponential decay model. Data traces, IRFs and fittings are shown in black, blue and red, respectively.

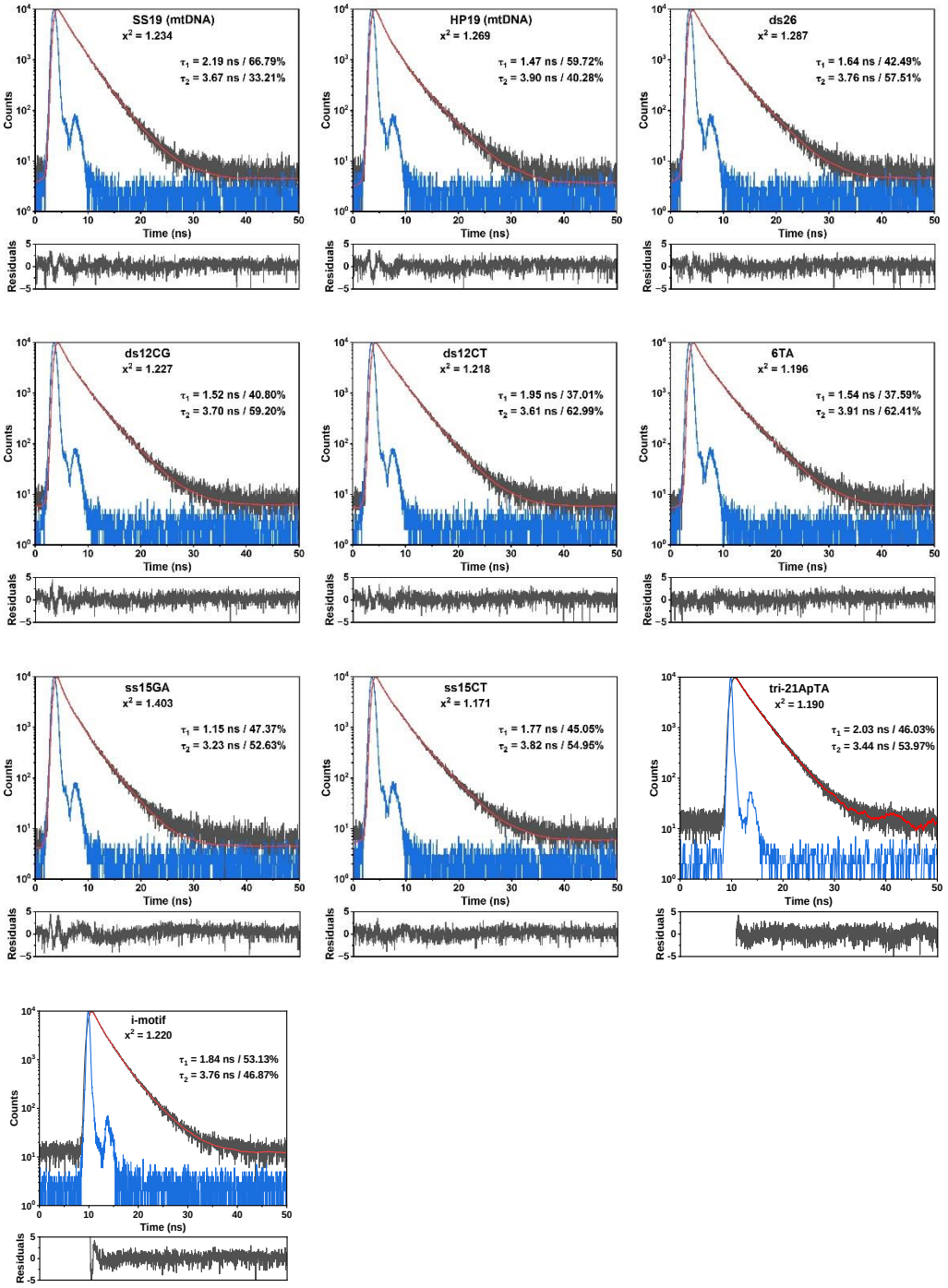

Figure S20. The fluorescence lifetimes (decays) of **TTPP** (1 μM) in the presence of different non-G4s DNA topologies in 10 mM Tris-HCl, 100 mM KCl, pH 7.4. All fittings are fitted to a bi-exponential decay model. Data traces, IRFs and fittings are shown in black, blue and red, respectively.

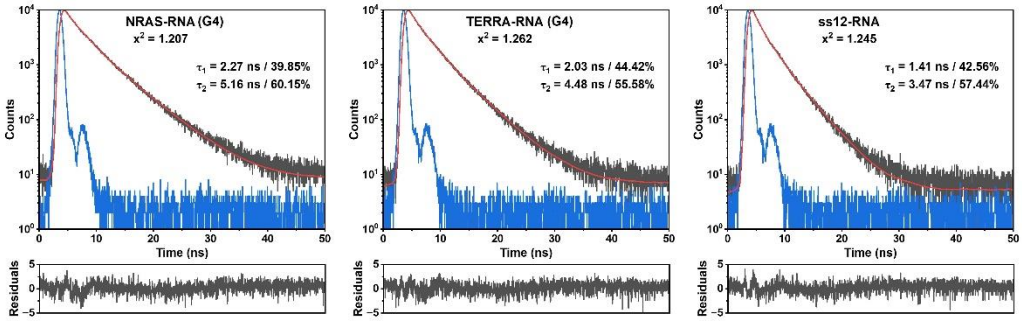

Figure S21. The fluorescence lifetimes (decays) of **TTPP** (1 μM) in the presence of different RNA topologies in 10 mM Tris-HCl, 100 mM KCl, pH 7.4. All fittings are fitted to a bi-exponential decay model. Data traces, IRFs and fittings are shown in black, blue and red, respectively.

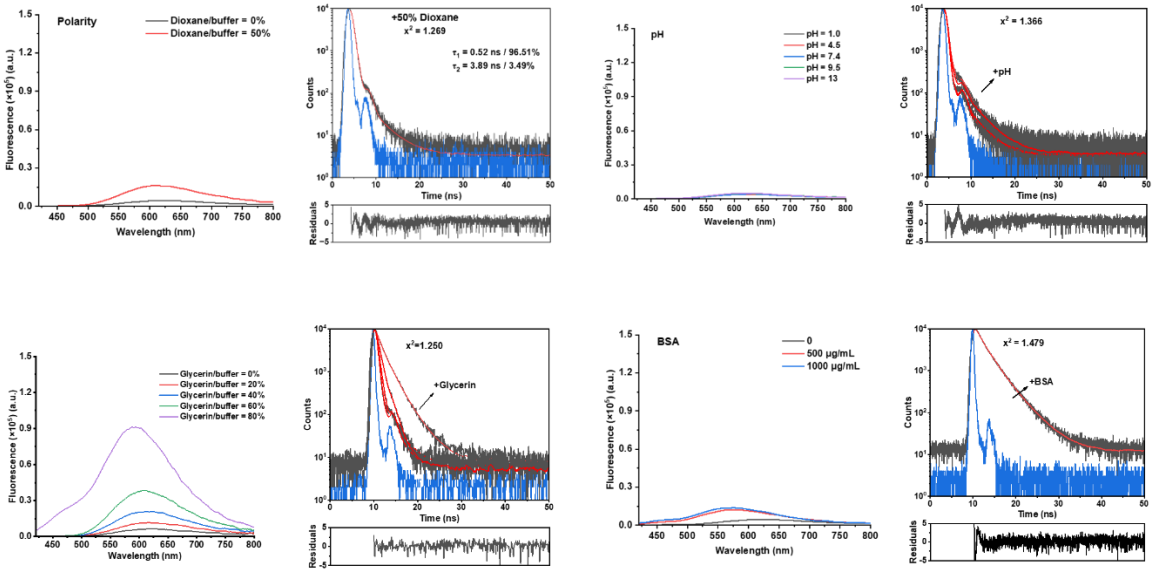

Figure S22. The effects of polarity, pH, viscosity and protein on the fluorescence properties (emission spectra and fluorescence lifetime) of **TTPP** (1 μM) at λ_{ex} = 405 nm in 10 mM Tris-HCl, 100 mM KCl, pH 7.4, respectively. The fitting is corresponding to a bi-exponential decay model. Data traces, IRFs and fittings are shown in black, blue and red, respectively.

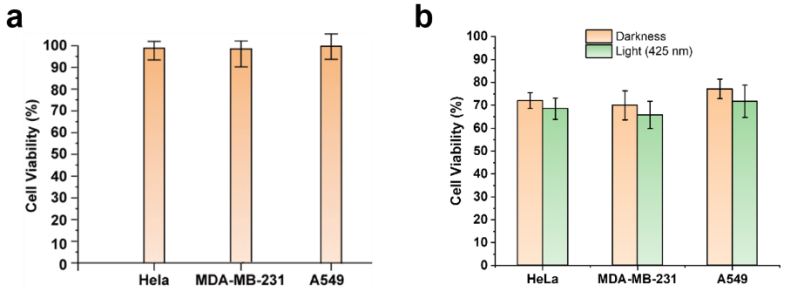

Figure S23. The cytotoxicity of **TTPP** probe tested by **MTT** assay. (a) Different cancer cells were incubated with **TTPP** (10 μM) for 24 hr under darkness. (b) Different cancer cells were incubated with **TTPP** (100 μM) for 48 hr under darkness/425 nm laser. Error bars are s.d. (n=3).

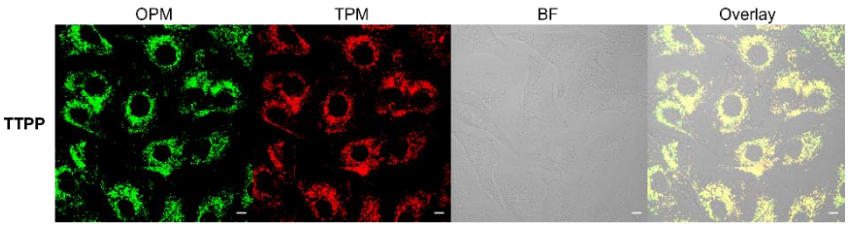

Figure S24. One-photon microscopy (OPM, λ_{ex} = 405 nm) and two-photon microscopy (TPM, λ_{ex} = 810 nm) images of **A549** cells incubated with 20 μM **TTPP** for 24 hours, respectively. Scale bars = 10 μm.

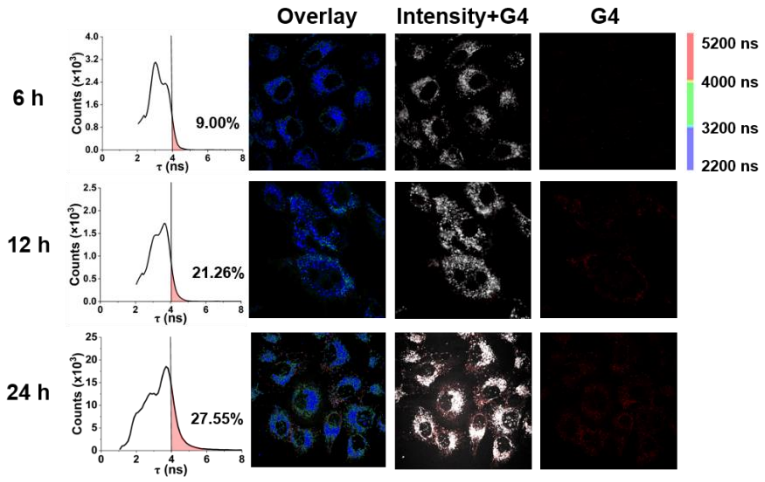

Figure S25. The FLIM images of A549 cells incubated with **TTPP** (10 μM) in 6, 12 and 24 hours.

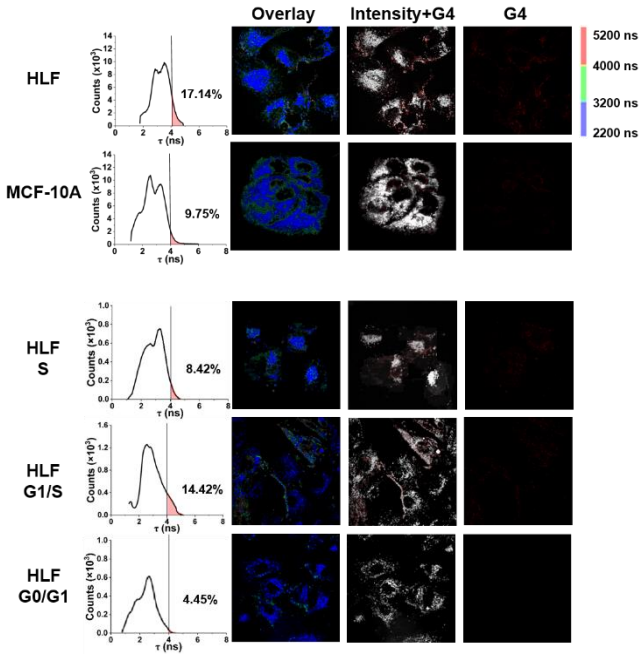

Figure S26. The FLIM images of HLF and MCF-10A cells incubated with **TTPP** (10 μM, 24 h) and the FLIM images of HLF cells at the G0/G1 and G1/S boundaries and during the S phase with **TTPP** (10 μM, 24 h).

Supplementary Table

Table S1. The nucleic acids sequences used in the study. [9]

Type	Name	Sequence（5’→3’）
mtDNA-G4s	Mito 27	AGGTCGGGGCGGTGATGTAGAGGGTGATGGT
	Mito 55	AGGGCGATGAGTGTGGGGAGGAATGGGGTGGGT
	Mito 141	GGGAGGATCCTATTGGTGCGGGGG
	Mito 143	GTGGGGTGAAAGAGTATGATGGGGTGGTGG
	Mito 165	GGGTGAGGGGTGGCTTTGGAGTTG
	Mito 0.5-22	GGTTAGGCGTACGGCCAGGGCTATTGG
	Mito 0.5-29	GGTTAGGTAGTTGAGGTCTAGGG
Other DNA-G4s	wtTel26	TTAGGGTTAGGGTTAGGGTTAGGGTT
	Tel26	AAAGGGTTAGGGTTAGGGTTAGGGAA
	MycG4	TGAGGGTGGGTAGGGTGGGTAA
	Myc1245	TTGGGGAGGGTTTTAAGGGTGGGGAAT
	MycA2A11	TAGGGAGGGTAGGGAGGGT
	VEGF-T12T13	CGGGGCGGGCCTTGGGCGGGGT
	VEGF-T12T13A2A21	CAGGGCGGGCCTTGGGCGGGAT
	BCL2	AGGGGCGGGCGCGGGAGGAAGGGGGCGGGAGCGGGGCTG
	BCL2-3T4AA	AGGGGCGGGCGCTTTAGGAAAAGGGCGGGA
	BCL2Mid	GGGCGCGGGAGGAATTGGGCGGG
	c-kit87up	AGGGAGGGCGCTGGGAGGAGGG
	c-kit2-G21T	CGGGCGGGCGCGAGGGAGGGT
	26CEB	AAGGGTGGGTGTAAGTGTGGGTGGGT
Non-G4 DNA	SS19 (mtDNA)	CAGTATCTGTCTTTGATTC
	HP19 (mtDNA)	CAGTATCTGTCTTTGATTCTTTTTTGAATCAAAGACAGATACTG
	ds26	CAATCGGATCGAATTCGATCCGATTG
	ds12CT	CTTTTGCAAAAG
	ds12CG	CGTGAATTCACG
	6TA	CGTACG
	ss15GA	GAAAAAAGAGAGAGG
	ss15CT	CTTTTTTCTCTCTCC
	tri-21ApTA	Ap21: AAAAAAAAAAAAAAAAAAAAA; T21: TTTTTTTTTTTTTTTTTTTT; A21: AAAAAAAAAAAAAAAAAAAAA
	i-motif	CCCTAACCCTAACCCTAACCCT
RNA	TERRA-RNA	UUAGGGUUAGGGUUAGGGUUAGGG
	NRAS-RNA	GGGAGGGGCGGGUCUGGG
	BCL2-RNA	GGGGGCCGUGGGGUGGGAGCUGGGG
	ds26-RNA	CAAUCGGAUCGAAUUCGAUCCGAUUG
	ss12-RNA	AUACGAUGCUUU

Table S2. The photophysical data of **TTPP** interacting with different DNA and RNA topologies in 10 mM Tris-HCl, 100 mM KCl, pH 7.40.

Type	**Number in Figure 1**	**Medium**	***Φ***	**τ_1 (ns) / f_1**	**τ_2 (ns) / f_2**
TTPP		none	0.07	0.2 / 98%	3.2 / 2%
mtDNA-G4s	5	Mito 27	0.55	1.7 / 32%	4.2 / 68%
	18	Mito 55	0.54	1.9 / 33%	4.5 / 67%
	6	Mito 141	0.52	1.9 / 43%	4.2 / 57%
	2	Mito 143	0.35	1.6 / 47%	4.1 / 53%
	11	Mito 165	0.51	1.9 / 30%	4.3 / 70%
	3	Mito 0.5-22	0.56	1.8 / 32%	4.1 / 68%
	4	Mito 0.5-29	0.57	1.8 / 29%	4.1 / 71%
Other DNA-G4s	15	wtTel26	0.54	2.2 / 26%	4.4 / 74%
	7	Tel26	0.56	2.1 / 28%	4.2 / 72%
	12	MycG4	0.47	1.7 / 33%	4.3 / 67%
	13	Myc1245	0.45	1.8 / 33%	4.3 / 67%
	21	MycA2A11	0.39	1.6 / 45%	4.9 / 55%
	16	VEGF-T12T13	0.40	1.7 / 35%	4.4 / 65%
	8	VEGF-T12T13A2A21	0.36	1.7 / 39%	4.2 / 61%
	9	BCL2	0.41	1.6 / 34%	4.2 / 66%
	10	BCL2-3T4AA	0.43	1.9 / 38%	4.2 / 62%
	14	BCL2Mid	0.42	1.6 / 35%	4.3 / 65%
	20	c-kit87up	0.45	1.9 / 35%	4.8 / 65%
	17	c-kit2-G21T	0.33	2.0 / 43%	4.4 / 57%
	1	26CEB	0.37	1.8 / 42%	4.0 / 58%
Non-G4 DNA	26	SS19 (mtDNA)	0.18	2.2 / 67%	3.7 / 33%
	30	HP19 (mtDNA)	0.17	1.5 / 60%	3.9 / 40%
	28	ds26	0.20	1.6 / 42%	3.8 / 58%
	25	ds12CT	0.31	2.0 / 37%	3.6 / 63%
	27	ds12CG	0.26	1.5 / 41%	3.7 / 59%
	31	6TA	0.19	1.5 / 38%	3.9 / 62%
	23	ss15GA	0.09	1.2 / 47%	3.2 / 53%
	29	ss15CT	0.23	1.8 / 45%	3.8 / 55%
RNA	19	TERRA-RNA (G4)	0.35	2.0 / 44%	4.5 / 56%
	22	NRAS-RNA (G4)	0.40	2.3 / 40%	5.2 / 60%
	24	ss12-RNA	0.10	1.4 / 43%	3.5 / 57%

Table S3. The photophysical data of **TTPP** in different pH, polarity, viscosity and protein in 10 mM Tris-HCl, 100 mM KCl, pH 7.40.

Type	Medium	Φ	τ_1 (ns) / f_1	τ_2 (ns) / f_2
TTPP	none	0.07	0.2 / 98%	3.2 / 2%
pH	1.0	0.09	0.1 / 98%	3.2 / 2%
	4.5	0.10	0.2 / 98%	3.2 / 2%
	7.4	0.07	0.2 / 97%	3.2 / 3%
	9.5	0.12	0.3 / 97%	3.4 / 3%
	13	0.11	0.3 / 98%	3.3 / 2%
Polarity	50% Dioxane	0.19	0.5 / 97%	3.9 / 3%
Viscosity	Glycerin/buffer = 20%	0.09	0.4 / 95%	3.3 / 5%
	Glycerin/buffer = 40%	0.15	0.5 / 97%	3.2 / 3%
	Glycerin/buffer = 60%	0.26	0.9 / 98%	3.3 / 2%
	Glycerin/buffer = 80%	0.40	1.4 / 67%	2.9 / 33%
Protein	BSA 500 μg/mL	0.09	0.8 / 37%	4.1 / 63%
	BSA 1000 μg/mL	0.10	1.1 / 36%	4.2 / 64%

Table S4. The representative docked free energies of the docking models between **TTPP** and DNA-G4 (Tel26).

The number of AutoDock clusters [a]	Docked free energy range of docked structures (kcal/mol)	Cluster rank [b]	Docked free energy (kcal/mol)
49 (50)	-11.87 to -4.26	1	-11.87
		2	-10.81
		3	-10.70
		4	-10.67
		5	-10.65
		6	-10.54
		7	-10.46
		8	-10.40
		9	-10.10
		10	-10.08

[a] The number of GA runs are shown in parentheses.

[b] The cluster rank is the absolute ranking as determined by the docked free energy defined by AutoDock.

Table S5. The representative docked free energies of the docking models between **TTPP** and duplex DNA (ds26).

The number of AutoDock clusters [a]	Docked free energy range of docked structures (kcal/mol)	Cluster rank [b]	Docked free energy (kcal/mol)
48 (50)	-12.08 to -5.93	1	-12.08
		2	-11.95
		3	-11.50
		4	-11.40
		5	-11.31
		6	-10.99
		7	-10.63
		8	-10.47
		9	-10.46
		10	-10.31

[a] The number of GA runs are shown in parentheses.

[b] The cluster rank is the absolute ranking as determined by the docked free energy defined by AutoDock.

References

[1] L. Y. Liu, W. Liu, K. N. Wang, B. C. Zhu, X. Y. Xia, L. N. Ji and Z. W. Mao, *Angew. Chem. Int. Ed.* **2020**, *59*, 9719-9726.

[2] M.-Q. Wang, Y. Wu, Z.-Y. Wang, Q.-Y. Chen, F.-Y. Xiao, Y.-C. Jiang, A. Sang, *Dyes Pigments* **2017**, *145*, 1-6.

[3] G.A. Reynolds, K.H. Drexhage, *Opt. Commun.* **1975**, *13*, 222-225.

[4] W. L. DeLano, *PyMOL(TM) Molecular Graphics System, Version 1.7* (Schrodinger, LLC, **2009**).

[5] C. I. Bayly, P. Cieplak, W. Cornell, P. A. Kollman, *J. Phys. Chem.* **1993**, *97*, 10269-10280.

[6] G. M. Morris, R. Huey, W. Lindstrom, M. F. Sanner, R. K. Belew, D. S. Goodsell, A. J. Olson, *J. Comput. Chem.* **2009**, *30*, 2785-2791.

[7] G. M. Morris, D. S. Goodsell, R. S. Halliday, R. Huey, W. E. Hart, R. K. Belew, A. J. Olson, *J. Comput. Chem.* **1998**, *19*, 1639-1662.

[8] Laskowski, R. *LigPlot*$^{+}$ *Version 1.4.5* (**2009**).

[9] a) J. Dai, C. Punchihewa, A. Ambrus, D. Chen, R. A. Jones, D. Yang, *Nucleic Acids Res.* **2007**, *35*, 2440-2450; b) J. Dai, M. Carver, C. Punchihewa, R. A. Jones, D. Yang, *Nucleic Acids Res.* **2007**, *35*, 4927-4940; c) A. Ambrus, D. Chen, J. Dai, R. A. Jones, D. Yang, *Biochemistry* **2005**, *44*, 2048-2058; d) R. I. Mathad, E. Hatzakis, J. Dai, D. Yang, *Nucleic Acids Res.* **2011**, *39*, 9023-9033; e) P. Agrawal, E. Hatzakis, K. Guo, M. Carver, D. Yang, *Nucleic Acids Res.* **2013**, *41*, 10584-10592; f) P. Agrawal, C. Lin, R. I. Mathad, M. Carver, D. Yang, *J. Am. Chem. Soc.* **2014**, *136*, 1750-1753; g) B. Onel, M. Carver, G. Wu, D. Timonina, S. Kalarn, M. Larriva, D. Yang, *J. Am. Chem. Soc*. **2016**, *138*, 2563-2570.